ELSEVIER

Journal of Power Sources 97–98 (2001) 97–103

JOURNAL OF POWER SOURCES

www.elsevier.com/locate/jpowsour

# Influence of edge and basal plane sites on the electrochemical behavior of flake-like natural graphite for Li-ion batteries

Karim Zaghib[a,*], Gabrielle Nadeau[a], Kimio Kinoshita[b]

[a]*Institut de Recherche d'Hydro-Québec, 1800 boul, Lionel-Boulet, Varennes, Que., Canada J3X 1S1*
[b]*Environmental Energy Technologies Division, Lawrence Berkeley National Laboratory, Berkeley, CA 94720, USA*

Received 28 June 2000; received in revised form 9 November 2000; accepted 23 December 2000

**Abstract**

The irreversible capacity loss (ICL) that is observed with carbons in Li-ion batteries is associated with electrolyte decomposition. In this paper, we present the results of an analysis to illustrate the role that the edge and basal plane sites play on the ICL and first-cycle coulomb efficiency of flake-like natural graphite. A model of an ideal graphite particle, which is depicted as an ideal prismatic structure, is used to develop an understanding of the correlation of the fraction of edge sites and particle size for flake-like and cube structures. In the case of flake-like graphite, thin flakes have higher surface area and higher ICL than thicker flakes, even though the fraction of edge sites is lower. On the other hand, the cube structure has a high fraction of edge sites but a low ICL and low surface area. The analysis presented here suggests that the particle morphology and the surface area associated with the edge and basal plane sites play a significant role in the electrochemical performance of graphite in Li-ion batteries. 

*Keywords:* Irreversible capacity loss (ICL); X-ray diffraction (XRD) analysis; Coulomb efficiency (CE)

## 1. Introduction

Carbon powders used in the negative electrodes of Li-ion batteries are available in a variety of particle morphologies, for example, flake-like (i.e. natural graphite), spherical (i.e. mesocarbon microbeads) and cylindrical (i.e. carbon fibers). Besides the particle morphology, other physicochemical properties of these carbons play a significant role in their electrochemical performance in Li-ion batteries. For instance, the degree of graphitization, particle size, surface area, relative surface fraction of edge and basal plane sites, microcavities, etc. affect the rate of intercalation/deintercalation, reversible capacity and the magnitude of the irreversible capacity loss (ICL).

One of the significant relationships observed by numerous researchers is that the ICL increases with an increase in the surface area of the carbon in the negative electrode [1–9]. This finding suggests that both the basal plane sites and edge sites on the carbon surface are effective sites for electrolyte decomposition. However, evidence is emerging that the catalytic activity of the carbon atoms at the basal and edge sites is different in their reactivity for electrolyte decomposition and the ICL [6–11]. These studies concluded that the edge sites are the more active (catalytic) sites for electrolyte decomposition. BarTow et al. [10] reported that the mechanism of electrolyte decomposition was different on the basal and edge sites in an electrolyte consisting of $LiAsF_6$ in ethylene carbonate (EC)-diethyl carbonate (DEC). The SEI layer formed on the edge sites is rich in inorganic compounds, whereas the SEI layer formed on the basal plane is rich in organic compounds. On the other hand, Yamamoto et al. [11] reported that no electrochemical reaction involving electrolyte decomposition occurred on the basal plane.

We have recently initiated studies to analyze the role of the edge and basal plane sites on the magnitude of the ICL on natural graphites for Li-ion batteries. The aim of this effort is to develop a better understanding of the contribution of these two distinct surface sites on graphite to the ICL. To conduct this investigation, graphite particles that consist solely of edge and basal plane surface sites is desired. Unfortunately, this ideal structure is not available. As an alternative, flake-like graphite powders of varying average sizes were used to simulate the ideal graphite structure. In this paper, we present the results of an analysis to illustrate the role that the edge and basal plane sites play on the electrochemical behavior of flake-like natural graphite. In this analysis, the

* Corresponding author. Tel.: +450-652-8019; fax: +450-652-8424.
*E-mail address*: karimz@ireq.ca (K. Zaghib).

0378-7753/01/$ – see front matter 
PII: S0378-7753(01)00596-1

electrochemical reaction involving the decomposition of the nonaqueous electrolyte during the initial charge (intercalation) of carbon, which is associated with the ICL, is investigated.

## 2. Experimental details

Five samples of flake-like natural graphite powders were obtained from a commercial source. These samples have average dimensions of 2, 12, 20, 30 and 40 μm in the direction parallel to the basal plane, and it is these dimensions that are referred to as the average particle size. Scanning electron microscopy (SEM, Hitachi) was employed to determine the morphology and dimensions of the edge and basal plane. X-ray diffraction (XRD) analysis (Siemens D500 Diffractometer) was used to determine the $d_{0\,0\,2}$ spacing and the crystallite size, $L_c$. The crystallite dimension, $L_a$, was obtained from Raman spectroscopy (argon-ion laser, Coherent Inc. Model Innova 70, tuned to 514.5 nm) by using the method of Tuinstra and Koenig [12], i.e. $L_a = 44/(I_{1372}/I_{1576})$, where $I_{1372}$ and $I_{1576}$ are the integrated intensities of the Raman peaks at 1372 and 1576 $cm^{-1}$, respectively. The Brunauer–Emmet–Teller (BET) surface area was measured with a Quantachrome Autosorb automated gas sorption system using $N_2$ gas.

Examples of the morphology of the natural graphite are shown in the SEM micrographs in Fig. 1. These micrographs illustrate the structure that is typical of the natural graphite flakes used in this study. It is apparent that a distribution of particle sizes is present in the sample, and the graphite particles consist predominantly of prismatic platelets with well-defined basal plan and edge dimensions. The edge thickness of the graphite particles was obtained from measurements of SEM micrographs of the graphite particles such as the ones in Fig. 1.

Electrochemical measurements of the charge/discharge of the natural graphite were conducted in an electrolyte containing 1 M $LiClO_4$ in 1:1 (volume ratio) ethylene carbonate (EC)-dimethyl carbonate (DMC) (Tomiyama Pure Chemical Industries Ltd.). The working electrode was fabricated from a mixture of the natural graphite and poly(vinylidene) fluoride (PVDF) dissolved in 1-methyl-2-pyrrolidinone (NMP). The slurry was spread onto a copper grid and dried

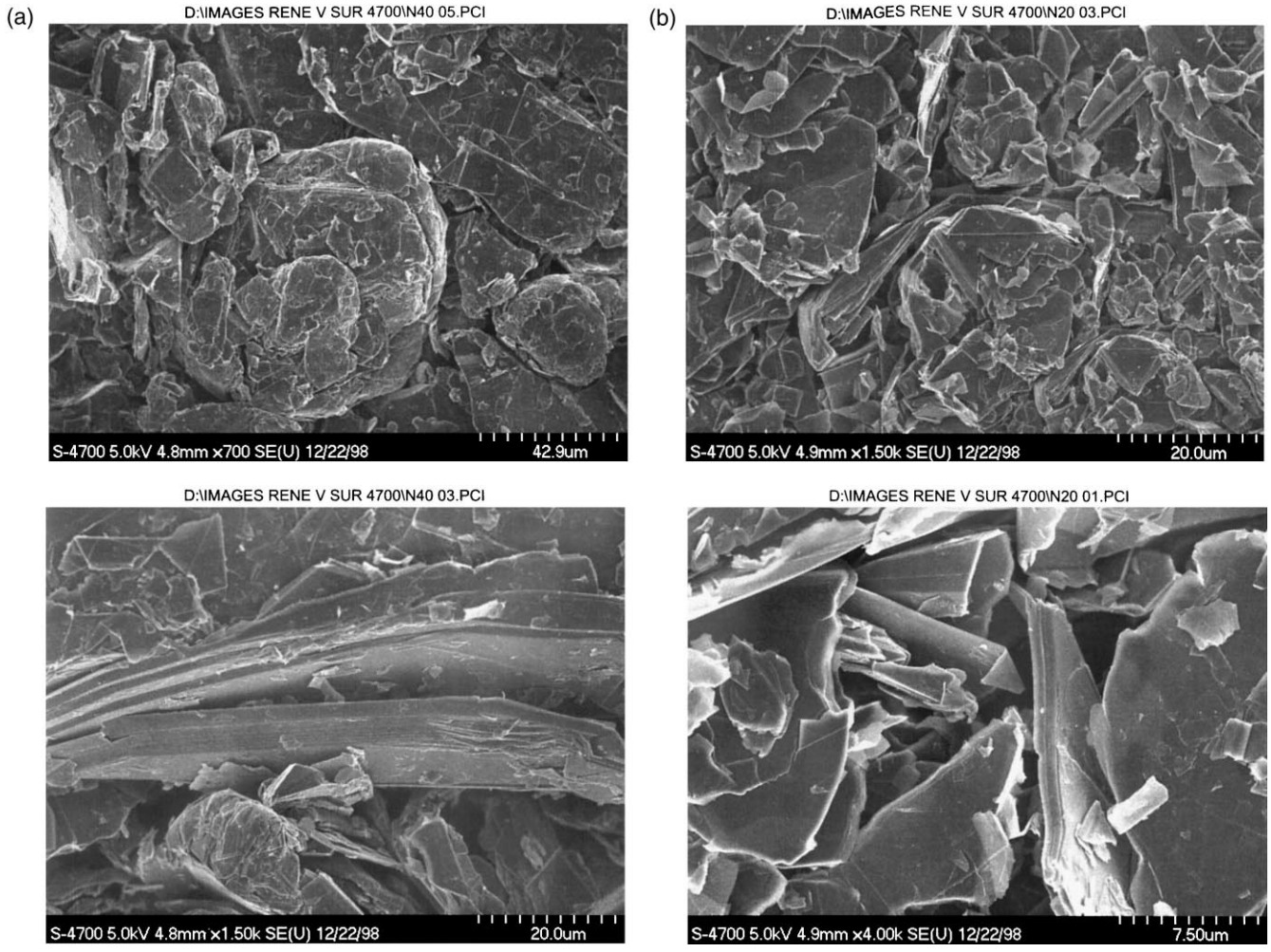


Fig. 1. SEM micrographs of natural graphite. Particle size: (a) 20 μm; (b) 40 μm.

under vacuum at 95°C for 24 h. The working electrodes were evaluated in a three-electrode cell that contained metallic Li as both counter and reference electrodes. The cells were assembled in a glove box under an Ar atmosphere containing less than 5 ppm humidity. The natural graphite samples were cycled at a *C*/24 rate between 2.5 and 0 V versus Li/$Li^+$ with a MacPile II (Bio Logic, France).

## 3. Discussion of results

### 3.1. Analysis of prismatic graphite structures

A model of an ideal graphite particle (see Fig. 2) was used to develop an understanding of the correlation of the fraction of edge sites and particle morphology. Two morphologies are represented in Fig. 2, flake-like and cube structure. Each of the particles is depicted as a collection of small prismatic crystallites that are arranged in a regular geometric pattern to form the desired model structure. The crystallites are arranged so that the particle consists of four edge and two basal plane surfaces. The relative fraction of carbon atoms at ende and basal plane sites was calculated to better understand their role in the electrochemical performance in negative electrodes for Li-ion batteries. This analysis utilized the equations reported by Fujimoto et al. [13,14] to calculate the number of carbon atoms in a crystallite and the particles. They derived a correlation between the size of the graphite crystallites and the crystallographic parameters, $L_a$, $L_c$, $d_{0\,0\,2}$ and $d_{1\,0\,0}$. The application of their correlation to our model of a graphite particle is described by Zaghib et al. [15]. The model graphite particle depicted in Fig. 2 consists of cubic crystallites that are arranged in a close-packed structure. In this model, edge atoms are present on the basal plane surface at intersections of adjoining crystallites. The graphite particle is assumed to have a regular prismatic

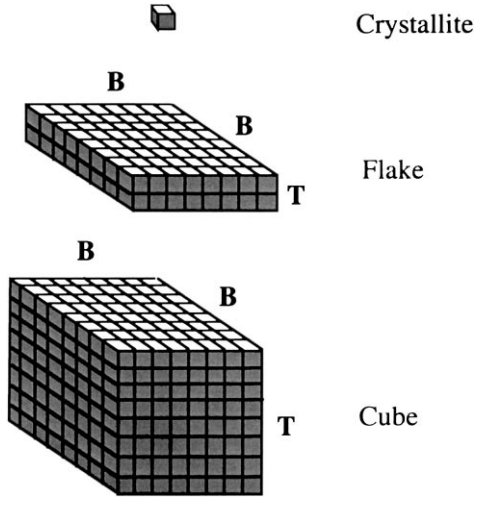


Fig. 2. Model structures for prismatic graphite particles and crystallite. Shaded area represents edge sites. *B* is the length of basal plane and *T* is the thickness of the edge plane.

structure with two adjustable parameters, the length of the basal plane (*B*) and the thickness of the edge plane (*T*). In the case where $B > T$, the prismatic structure resembles the flake-like graphite structure, and when $B = T$, the prismatic structure is a cube. One limiting case is when $L_a \gg d_{100}$ and $L_c \gg d_{002}$, which is reasonable for natural graphite. In this situation, the surface fraction of edge atoms ($f_e$) is given by

$$f_e = \frac{2B/L_a + T/d_{002}}{2B/d_{100} + T/d_{002}} \quad (1)$$

It is evident from Eq. (1) that $f_e$ is a function of crystallographic parameters, $d_{0\,0\,2}$ and $L_a$, that are characteristic of the edge and basal plane dimensions, respectively. An increase in $L_a$ is associated with an increase in the dimension of the basal plane. An expansion in $d_{0\,0\,2}$ results in a lower number of carbon atoms per unit area of the edge plane sites.

The fraction of edge surface sites can also be simply determined from the dimensions of the flake-like structure. In this case the fraction of edge sites is given by

$$f'_e = \frac{2T}{B + 2T} \quad (2)$$

However, this relationship does not take into account the fact that the geometric arrangement of the carbon atoms on the edge and basal plane surfaces are different. The carbon atoms at the termination of the edge planes are separated by a much larger distance (e.g. 3.354 Å in graphite) than the atoms in the basal plane (in-plane C–C distance is 2.461 Å). Thus, $f_e$ is much lower than $f'_e$ when this fact is taken into account, as opposed to the situation where only the geometric distances are considered. In the following analysis, $f_e$ determined by Eq. (1) will be used. The surface area of the model graphite particle, *S* ($m^2$/g), is computed from the geometric dimensions

$$S = \frac{2(B + 2T)}{\rho BT} \quad (3)$$

where $\rho$ is the density. This value can be compared to the BET surface area, SBET, which considers adsorption on essentially a smooth surface.

The two-dimensional prismatic flake-like structure with $B \gg T$, and the three-dimensional cube structure with $B = T$, are representative of the particle morphology that resembles the flake-like natural graphite and MCMB, respectively. Eq. (1) was used to analyze the change in the fraction of edge sizes for the flake-like structure as a function of its particle size (*B*). For this analysis, it is assumed that $L_a = L_c = 100$ Å, $d_{002} = 3.36$ Å and $\rho = 2.25$ g/$cm^3$. The change in $f_e$ as a function of particle size is plotted in Fig. 3 for the flake-like structures with edge thickness (*T*) of 0.2, 1 and 2 μm. It is apparent that the thicker flake structure has a higher $f_e$ than that of a thinner flake. Furthermore, $f_e$ gradually decreases with an increase in *B*. The value of $f_e$ for the different flakes diminishes as *B* becomes larger because the basal plane area dominates, $B \gg T$, and the area of the edge sites becomes very small.

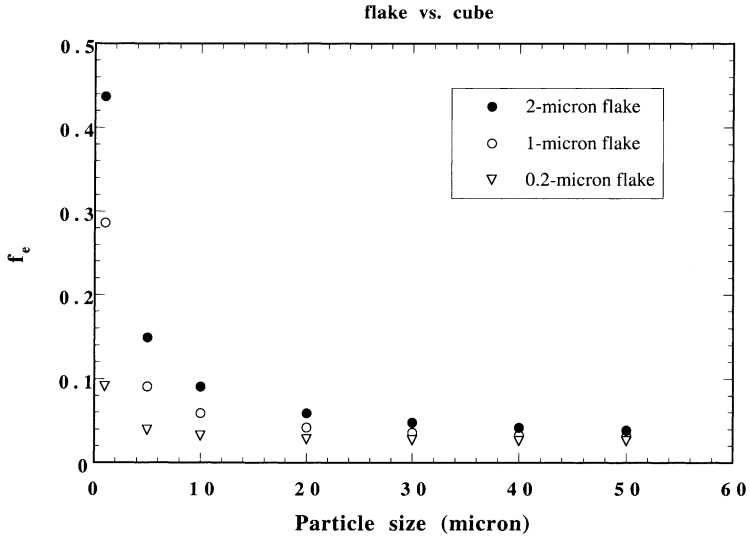


Fig. 3. Change in $f_e$ as a function of particle size of flake-like structure: $T = 0.2$, 1 and 2 μm.

For the cube structure with $B = T$, $f_e$ is a constant ($f_e = 0.286$), independent of particle size because both $B$ and $T$ change in the same manner. The changes in surface area of the flake-like and cube-like structures are presented in Fig. 4. As expected, the flake and cube structures with the smallest dimensions have the highest surface area. The surface area of the flake-like structure with $T = 0.2$ μm is considerable greater than those of the other flake and cube structures (1999 lists numerous examples).

### 3.2. Comparison of model structure and flake-like natural graphite

The series of natural graphite samples used in the present study provides a range of particle sizes of prismatic geometry from which the edge-site concentration is estimated. The physical properties of the natural graphite particles are reported elsewhere [13]. In brief, the BET surface area decreased from 12.1 to 2.3 $m^2/g$ with an increase in the average particle size from 2 to 40 μm. The corresponding thickness of the edge planes increased from 0.21 to 2.85 μm with an increase in the particle size. The results obtained from Raman spectroscopy indicate $L_a$ is in the range from 110 to 183 Å. X-ray diffraction analysis showed that the $d_{0\,0\,2}$ spacing is 3.36 Å, and $L_c$ ranges from 54 to 80 Å. Typically, natural graphite has crystallite dimension $L_c$ that are considerably higher (i.e. about 1000 Å) that those reported here. However, graphites with $d_{0\,0\,2}$ spacing near 3.36 Å are available with much lower $L_c$. For instance, US Patent 5,882,818 (issued 16 March, 1999) lists numerous

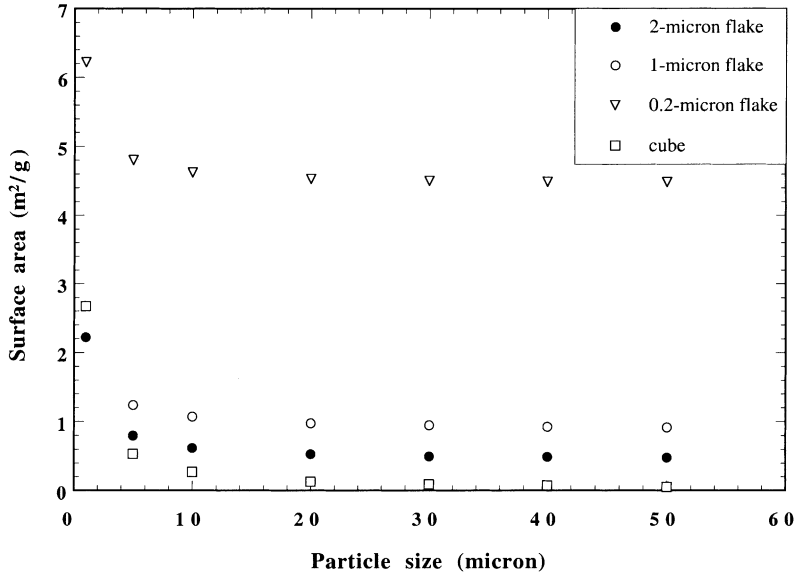


Fig. 4. Change in $f_e$ as a function of particle size of flake-like structure with $T = 0.2$, 1 and 2 μm and cube-like structure.

examples of graphites with similar $d_{0\,0\,2}$ spacing that have $L_c < 200$ Å. It is these types of natural graphite that were used in our study.

The electrochemical results for the first cycle intercalation and deintercalation of Li in natural graphite particles were compared to the theoretical predictions obtained for the flake-like and cube structures. For the model structures, we assume that the total irreversible capacity loss ($ICL_t$) consists of contributions from the basal plane ($ICL_b$) and edge sites ($ICL_e$), i.e.

$$ICL_t = ICL_b + ICL_e \quad (4)$$

The ICL of the surface sites $i$ ($i$ = edge sites or basal plane sites), expressed in mAh/g, is given by

$$ICL_i = k_i S_i \quad (5)$$

and it follows that

$$ICL_e = k_e S_e \quad (6)$$

$$ICL_b = k_b S_b \quad (7)$$

where $k_e$ and $k_b$ are constants that are a function of the reactivity of the surface site for electrolyte decomposition. The surface area associated with the edge and basal planes sites is estimated by use of Eqs. (1) and (3). The surface area of edge and basal plane sites are given by

$$S_e = f_e S \quad (8)$$

and

$$S_b = (1 - f_e) S \quad (9)$$

respectively. The contributions from the basal plane and edge sites to $ICL_t$ are derived from the results reported by Chung et al. [7]. They determined the irreversible capacity loss on a variety of carbons (e.g. natural and artificial graphite, mesocarbon microbeads, carbon fibers), from which the irreversible capacity loss per surface area on the basal plane ($q_b$) and edge ($q_e$) sites were estimated, i.e. $q_b = 5.5$ mAh/m$^2$ and $q_e \geq 35$ mAh/m$^2$ for flaky graphite. Therefore, the analysis of the role of surface sites on electrolyte decomposition should account for the catalytic activity of the basal plane as well as the edge sites. From the values reported by Chung et al., the irreversible capacity loss per surface area of edge sites is 7.4 times greater than that on the basal plane ($k_e = 7.4 k_b$). This result allowed us to calculate the contribution of the two types of surface sites to the total irreversible capacity loss.

The ICL that was calculated for the model structures and the experimental data obtained for natural graphite is plotted in Fig. 5 as a function of surface area. The surface area of the model structures was determined with the use of Eq. (3), and the BET surface area is used for the natural graphite samples. With the exception of the calculated ICL values for small particle size ($B < 5$ μm), the trend line shows a linear relationship between ICL and surface area. This relationship is commonly observed for carbon in the negative electrode of Li-ion batteries [1–9]. Closer inspection of the results in Fig. 5 indicates that differences exist in the slope of the data for the different flake and cube structures, indicating the contribution of the relative fraction of edge and basal plane sites on the total ICL. The 2 μm flake has a proportionally higher fraction of edge sites than the other flake-like structures, and consequently its change in ICL with surface area is much greater.

The calculated ICL for the flake-like and cube structures are plotted in Fig. 6 as a function of the particle size, along with the experimental results obtained with natural graphite. The ICL for the 0.2 μm flake particles is considerable greater

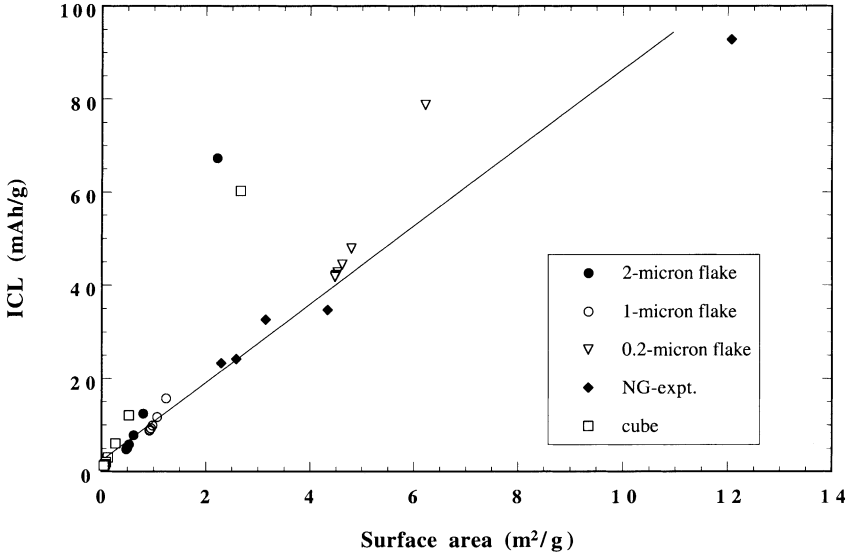


Fig. 5. Influence of particle size on ICL. Calculated values for flake-like and cube structures and experimental results obtained with natural graphite (NG). Line shows the trend of experimental data.

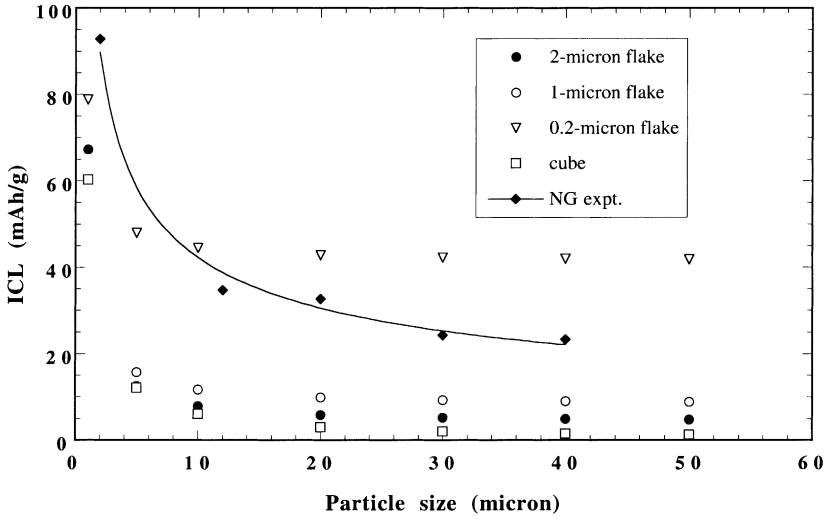


Fig. 6. Relationship between ICL and surface area for model particle structures and natural graphite. Line shows trend of the data.

than the corresponding values for the larger flake particles and cube structure. This difference is a consequence of the much higher surface area of the thinner flakes (see Fig. 4), because the relative fraction of edge sites is less than that of the larger particles (see Fig. 3). On the other hand, the cube structure shows a smaller ICL than the flake-like structures even though the fraction of edge sites is much larger for particle sizes of about 5 μm or greater. In this case, the surface area of the cube structure for a given particle size is less than that for the flake-like structure. These results suggest that the basal plane surface can contribute significantly to the total ICL. The experimental results obtained with natural graphite are also plotted in Fig. 6. Because the physical properties of these natural graphite samples are not constant (i.e. $T$ and $L_a$ vary with $B$, particle morphology is not an ideal flake-like structure), the ICL does not agree very well with the calculated values for the model flake-like structure. However, the trend of the experimental data appears to fall between the results for the 0.2 and 1 μm flakes.

The first cycle coulomb efficiency (CE) for intercalation/de-intercalation of $Li^+$ ions in carbon electrodes is given by

$$\mathrm{CE} = \frac{\mathrm{RC}}{\mathrm{RC} + \mathrm{ICL_t}} \tag{10}$$

where RC is the reversible capacity for Li intercalation, and it is assumed to be equal to 372 mAh/g. The coulomb efficiency calculated from Eq. (5) for the flake-like and cube structures are plotted in Fig. 6 as a function of particle size. A high CE (>0.97) is obtained with the 2 and 1 μm flake-like particles and the cube structure when the reversible capacity is high, for example, equivalent to 372 mAh/g. The cube structure shows the highest CE because of its low ICL, and the small flake-like structure has the highest CE, consistent with the high ICL. The experimental results obtained with the natural graphite are also plotted in Fig. 7. The trend of the data, which is indicated by the solid line, shows that the natural graphite has CE slightly higher than the 0.2 μm flake structure.

Based on the analysis described in this paper, we conclude that the surface area associated with the edge sites, and not the total BET surface area, has the dominant influence on the irreversible capacity loss and coulomb efficiency of carbons for Li-ion batteries. The crystallite parameters, $L_a$ and $L_c$, and the $d_{0\,0\,2}$ spacing change with heat treatment of graphitizable carbons. The crystallite parameters increase, and the $d_{0\,0\,2}$ spacing decreases, with increasing heat-treatment temperature. Furthermore, the change in these parameters with heat treatment will vary with the carbon precursor. The increase in $L_c$ and decrease in $d_{0\,0\,2}$ spacing will also reduce the relative amount of edge sites present in graphitizable carbons. Consequently, heat treatment is a viable option for controlling the physical properties of graphitizable carbons and their ICL in Li-ion batteries.

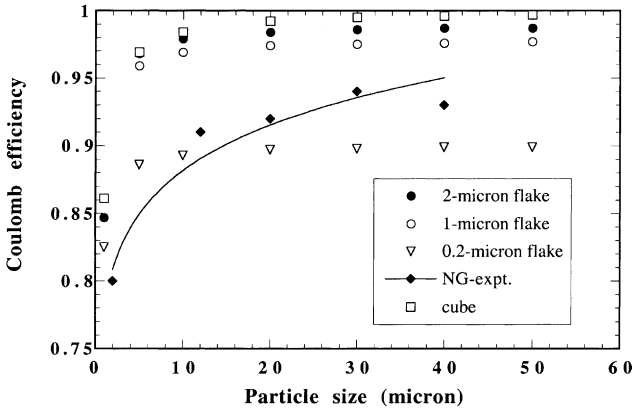


Fig. 7. Influence of particle size on coulomb efficiency. Calculated values for flake-like and cube structures and experimental results obtained with natural graphite (NG). Line shows the trend of experimental data.

## 4. Concluding remarks

The simple analysis presented here suggests that the particle morphology and the relative fraction of edge and basal plane sites play a significant role in the electrochemical performance of graphite in Li-ion batteries. In the case of flake-like graphite, thin flakes have higher surface area and consequently higher ICL. Despite the fact that thin flakes have a large fraction of basal plane sites, their contribution to the ICL is still significant. On the other hand, the cube structure has a high fraction of edge sites but a low ICL. This behavior is due to the low surface area of the cube structure. Based on the analysis of the two different prismatic structures, flake-like versus cube, the latter particle morphology appears to offer an advantage in electrochemical performance. That is, the cube structure has a lower ICL and higher CE than flake-like particles of comparable size. Although no evidence is presented, with the morphology of the cube structure as presented here, the high fraction of edge sites ($f_e = 0.286$) should be beneficial for obtaining high rates of $Li^+$-ion intercalation/de-intercalation. Thus, three-dimensional graphite particles such as a cube structure are well-suited for high-rate applications in Li-ion batteries. In this regard, MCMBs which are most closely comparable to three-dimensional graphite particles show promise for high-rate applications [16,17].

## Acknowledgements

The authors would like to acknowledge the support of HydroQuebec and the Assistant Secretary for Energy Efficiency and Renewable Energy, Office of Advanced Automotive Technologies of the US Department of Energy under Contract No. DE-AC03-76SF00098 at Lawrence Berkeley National Laboratory. The Raman measurements by Dr. Robert Kostecki is gratefully acknowledged.

## References

[1] R. Fong, U. von Sacken, J. Dahn, J. Electrochem. Soc. 137 (1990) 2009.
[2] F. Disma, L. Aymard, L. Dupont, J. Tarascon, J. Electrochem. Soc. 143 (1996) 3959.
[3] K. Takei, N. Terada, K. Kumai, T. Iwahori, T. Uwai, T. Miura, J. Power Sources 55 (1995) 191.
[4] M. Terasaki, H. Yoshida, T. Fukunaga, H. Tukamoto, M. Mizutani, M. Yamachi, GS News Tech. Rep. 53 (1994) 23.
[5] Barsoukov, J. Kim, C. Yoon, H. Lee, J. Electrochem. Soc. 145 (1998) 2717.
[6] M. Winter, P. Novak, A. Monnier, J. Electrochem. Soc. 145 (1998) 428.
[7] G.-C. Chung, S.-H. Jun, K.-Y. Lee, M.-H. Kim, J. Electrochem. Soc. 146 (1999) 1664.
[8] T. Tran, B. Yebka, X. Song, G. Nazri, K. Kinoshita, D. Curtis, J. Power Sources 85 (2000) 269.
[9] E. Peled, D. Bar-Tow, A. Melman, E. Gerenrot, Y. Lavi, Y. Rosenberg, in: N. Doddapaneni, A. Landgrebe (Eds.), Proceedings of the Symposium on Lithium Batteries, Vol. 94-4, The Electrochemical Society, Inc., Pennington, NJ, 1994, p. 177.
[10] D. BarTow, E. Peled, L. Burstein, J. Electrochem. Soc. 146 (1999) 824.
[11] O. Yamamoto, Y. Takeda, N. Imanishi, in: B. Barnett, E. Dowgiallo, G. Halpert, Y. Matsuda, Z. Takehara (Eds.), Proceedings of the Symposium on New Sealed Rechargeable Batteries and Supercapacitors, PV 93-23, The Electrochemical Society, Inc., Pennington, NJ, 1993, p. 302.
[12] F. Tuinstra, J. Koenig, J. Chem. Phys. 53 (1970) 1126.
[13] H. Fujimoto, A. Mabuchi, K. Tokumitsu, T. Kasuh, N. Akuzawa, Carbon 32 (1994) 193.
[14] H. Fujimoto, K. Tokumitsu, A. Mabuchi, T. Kasuh, M. Shiraishi, Carbon 32 (1994) 1249.
[15] K. Zaghib, G. Nadeau, K. Kinoshita, J. Electrochem. Soc., accepted for publication.
[16] R. Gitzendanner, P. Russell, C. Marsh, R. Marsh, J. Power Sources 81/82 (1999) 847.
[17] S. Ahn, Y. Kim, K. Kim, T. Kim, H. Lee, M. Kim, J. Power Sources 81/82 (1999) 896.